

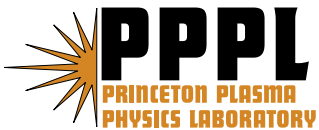
PPPL-4240

PPPL-4240

**Enhanced Performance  
of Cylindrical Hall Thrusters**

Y. Raitses, A. Smirnov, and N.J. Fisch

May 2007



# Princeton Plasma Physics Laboratory

## Report Disclaimers

---

### Full Legal Disclaimer

This report was prepared as an account of work sponsored by an agency of the United States Government. Neither the United States Government nor any agency thereof, nor any of their employees, nor any of their contractors, subcontractors or their employees, makes any warranty, express or implied, or assumes any legal liability or responsibility for the accuracy, completeness, or any third party's use or the results of such use of any information, apparatus, product, or process disclosed, or represents that its use would not infringe privately owned rights. Reference herein to any specific commercial product, process, or service by trade name, trademark, manufacturer, or otherwise, does not necessarily constitute or imply its endorsement, recommendation, or favoring by the United States Government or any agency thereof or its contractors or subcontractors. The views and opinions of authors expressed herein do not necessarily state or reflect those of the United States Government or any agency thereof.

### Trademark Disclaimer

Reference herein to any specific commercial product, process, or service by trade name, trademark, manufacturer, or otherwise, does not necessarily constitute or imply its endorsement, recommendation, or favoring by the United States Government or any agency thereof or its contractors or subcontractors.

---

## PPPL Report Availability

### Princeton Plasma Physics Laboratory:

<http://www.pppl.gov/techreports.cfm>

### Office of Scientific and Technical Information (OSTI):

<http://www.osti.gov/bridge>

---

### Related Links:

[U.S. Department of Energy](#)

[Office of Scientific and Technical Information](#)

[Fusion Links](#)

## **Enhanced performance of cylindrical Hall thrusters**

Y. Raitses,<sup>a)</sup> A. Smirnov, N. J. Fisch  
Princeton Plasma Physics Laboratory  
Princeton, NJ 08543

### **ABSTRACT**

The cylindrical thruster differs significantly in its underlying physical mechanisms from the conventional annular Hall thruster. It features high ionization efficiency, quiet operation, ion acceleration in a large volume-to-surface ratio channel, and performance comparable with the state-of-the-art conventional Hall thrusters. Very significant plume narrowing, accompanied by the increase of the energetic ion fraction and improvement of ion focusing, led to 50- 60% increase of the thruster anode efficiency. These improvements were achieved by overrunning the discharge current in the magnetized thruster plasma.

<sup>a)</sup> Electronic address: [yraitses@pppl.gov](mailto:yraitses@pppl.gov)

The demonstration of highly efficient ( $\geq 50\%$ ) medium and high power Hall thrusters<sup>1,2</sup> now motivates efforts toward developing miniaturized Hall thrusters<sup>3-5</sup> for low power space applications. The annular design of the conventional Hall thrusters, however, does not naturally lend itself to scaling to small size because of the large surface-to-volume ratio and the difficulty in miniaturizing the magnetic circuit.<sup>3</sup> The efficiency tends to be lower (6-30%),<sup>3,5</sup> plasma divergence larger,<sup>4</sup> and the lifetime issues, including heating and erosion of the thruster parts,<sup>3,4</sup> become more aggravated. Alternative approaches to low power scaling exploit different  $E \times B$  configurations, including outside electric field thruster,<sup>6</sup> linear<sup>7</sup> and cylindrical<sup>5,8</sup> Hall thrusters. With the advent of the cylindrical Hall thruster (CHT) concept,<sup>8</sup> several thruster designs<sup>5,9,10</sup> have been developed and studied. A typical CHT features high ionization efficiency,<sup>8,9,11</sup> quiet operation,<sup>5,8,9</sup> ion acceleration in a small surface-to-volume ratio channel,<sup>8,9,12</sup> and performance comparable with the state-of-the-art annular Hall thrusters of similar sizes.<sup>5,8,9</sup> In this letter, we report that narrowing of the plasma plume in the miniaturized CHT leads to the highest performance at 100 W power level.

The principle of operation of the CHT (Fig. 1) is described in detail elsewhere.<sup>5,8,12</sup> It is in many ways similar to that of a typical annular Hall thruster,<sup>1</sup> i.e., it is based on a closed  $E \times B$  electron drift in quasineutral plasma. However, in contrast to the conventional annular geometry, in the cylindrical geometry the axial potential distribution is now critical for electron confinement. This is because the electrons are not confined to an axial position; rather they bounce over an axial region impeded from entering the anode by the magnetic mirror.<sup>12</sup>

One of the key drawbacks of existing CHTs is the unusually large beam divergence of the plasma plume. The plasma plume angle is usually defined as the angle that contains not less than 90% of the total ion current.<sup>2,15</sup> For the CHTs, the half plume angle can be as large as 60-80°,<sup>8</sup> compared to 45-50° for the state-of-the art annular Hall thrusters.<sup>2</sup> For the annular Hall thrusters, the beam divergence is due to the combined effect of radial pressure gradients, magnetic field curvature, and the non-uniform distribution of the ion production.<sup>13, 14</sup> Controlling the placement and length of the ion acceleration region using segmented electrodes<sup>15</sup> or by optimizing the magnetic field topology<sup>2,13</sup> were shown to narrow the plasma plume in the annular thrusters. However, in the CHT case, the magnetic field topology is very different from conventional Hall thrusters, and, therefore, the means of controlling the plume divergence may be very different. In the present work, by overrunning the discharge current, a very dramatic plume narrowing is demonstrated for two miniaturized cylindrical thrusters.

Two laboratory CHTs of different diameters, 2.6 cm and 3 cm, were built to operate at the 100 W power level. For the 2.6 cm CHT, details of the design and results of comprehensive experimental and numerical studies are described elsewhere.<sup>5,11,12</sup> Both thrusters have the same longitudinal channel dimensions and comparable magnetic field topologies. In the present experiments, we conducted plume and thrust measurements. A commercial hollow cathode was used as a cathode-neutralizer.<sup>8,11,12</sup> During the plume measurements, the background pressure in a 28 m<sup>3</sup> vacuum vessel equipped with cryopumps<sup>15</sup> did not exceed 3 microtorr. The thrust-stand, thrust

measurement procedures, and experimental uncertainties are described in detail elsewhere.<sup>5</sup> In these experiments, the background pressure was about 5 microtorr.

The plume diagnostic tools were placed at the distance of 72 cm from the channel exit and rotated  $\pm 90^\circ$  relative to the thruster axis. The ion angular distribution (Fig. 2) was measured using a negatively biased planar probe with a guarding sleeve. A two-grid retarding potential analyzer (RPA) was used to measure the ion energy distribution function (IEDF) at different angular locations (Fig. 3). The overall transparency of RPA grids is  $\approx 16\%$ . The angular distribution for different energy ions was also measured during the rotation of the RPA with a constant bias voltage,  $V_{RPA}$ , applied to the ion retarding grid. Under such conditions, the RPA is transparent only for ions with the energy,  $\epsilon_{ion} > eV_{RPA}$ . The ion current was measured by a picoammeter. The angular distribution of the ion current measured with the RPA at  $V_{RPA} = 0$  V approximately coincides with the current distribution measured by the ion flux probe (Fig. 2). The total ion flux was obtained by integrating the measured angular distribution of the ion current measured by the probe and by the RPA (for ions with  $\epsilon_{ion} > eV_{RPA}$ ). The total ion current was used to determine the current utilization<sup>1,2,12</sup> (the ratio of the ion current to the discharge current), which characterizes magnetic insulation of the thruster discharge. Finally, the thruster efficiency,  $\eta = T^2 / 2\dot{m}P_e$ , was deduced from measurements of the thrust,  $T$ , discharge power,  $P_e$ , and the anode mass flow rate,  $\dot{m}$ . Here, the additional gas flow rate through the cathode (2-3 sccm) is not taken into account. The key result of this study is that, by increasing the discharge current over and above what is normally required for sustaining the steady state

discharge (at given gas flow rate, discharge voltage and magnetic field), we now achieve a dramatic (20-30%) plume narrowing (Fig. 2), a substantial increase (50-60%) of the thruster anode efficiency at 100-200 W (Fig. 4) and efficient plasma production and ion acceleration (anode efficiency of 30-40%) at the lower discharge power.

The discharge power is the discharge voltage times the discharge current. It does not take into account the additional power, which was used to overrun the discharge current. This is because this additional power is somewhat arbitrary since it was not minimized in the present experiments. Such a non-self-sustained thruster operation can be realized in different ways such as, for example, by driving the current between the segmented electrodes<sup>15</sup> and the cathode or between the keeper electrode and the emitter of the cathode-neutralizer. The latter approach was used in the present work. Fig. 3 shows that the peak ion energy is shifted ( $\sim 30$  eV) towards higher ion energies in the overrun current regime. This effect can be partially explained by a reduced cathode voltage drop required to sustain the thruster discharge at low currents.<sup>16</sup>

For the 2.6 cm CHT operated at the discharge voltage of 250 V and the anode gas flow rate of 4 sccm, the maximum reduction of a half plume angle was almost  $20^\circ$  (from  $74^\circ$  to about  $55^\circ$ ), when the discharge current was increased from 0.57A to 0.66A. Because the ion current also increases, the current utilization changes insignificantly, from 73% to 71%. For the same operating conditions, the 3 cm CHT can produce an even narrower plume than the smaller CHT: half plume angle reduced from  $62^\circ$  to  $50^\circ$ .

This reduction was accompanied by a reduction of the current utilization from about 71% to 66%. Differences in the operation of the miniaturized CHTs and the additional power used to overrun the discharge current ( $\sim 20$  W) may explain the smaller reduction of the plume angle and the stronger degradation of the magnetic insulation obtained for the larger thruster. Indeed, the 3 cm CHT operation was not in an optimal regime, but rather adjusted (through the magnetic field) to be comparable with the operating parameters of the 2.6 cm CHT. In addition, in the normal operating regime, the 3 cm CHT already produces a narrower plume, so any further reduction in plume angle becomes harder to realize. Note that this reduced plume angle is comparable to a typical plume angle reported for high performance annular Hall thrusters.<sup>2,15</sup>

Apparently, a nearly twofold increase in the fraction of high-energy ions (Fig. 5a), better focusing of these ions (Fig. 5b), and a shift of IEDF toward higher energies (Fig. 3) contributed to the increase of the thrust and, as a result, the thruster efficiency (Fig. 4) in the non self-sustained thruster regime with the overrun discharge current. An important observation of the most recent experiments is that the additional power required to overrun the discharge current can be reduced from 20-50 W to several watts without a degradation of the plasma plume. Although the overrun current effect on the CHT plasma is dramatic, leading to extraordinary efficiencies in several thruster variations, it remains to understand in detail the physics of this effect and the ways to optimize it.

The authors would like to thank Mr. Erik Granstedt and Dr. Leonid Dorf for their technical assistance and valuable discussions. The authors gratefully acknowledge Professor Edgar Choueiri of the Princeton University for the use of the EPPDyL thrust stand. This research was supported by the Air Force Office of Scientific Research.

## References

1. V. Kim, J. Prop. Power 14, 736 (1998).
2. R. R. Hofer and A.D. Gallimore, J. Prop. Power 22, 748 (2006).
3. V. Khayms and M. Martinez-Sanchez, in Progress in Astronautics and Aeronautics, vol. 187, p. 45, edited by M.M. Micci and A.D. Ketsdever. AIAA, Reston, VA, 2000.
4. T. Ito and M. A. Cappelli, Appl. Phys. Lett. 89, 061501 (2006); T. Ito, N. Gascon, W. Crawford and M. Cappelli, *Proceedings of 42nd Joint Propulsion Conference and Exhibit, July 2006, Sacramento, CA* (American Institute of Aeronautics and Astronautics, Reston, VA 2002), AIAA paper No. 2006-4495.
5. A. Smirnov, Y. Raitses, and N. J. Fisch, J. Appl. Phys. 92, 5673 (2002).
6. A. M. Kapulkin, A. D. Grishkevich and V. F. Prisnyakov, Proceedings of the 45 Inter. Astron. Federation Congress, Jerusalem, Israel, October 1994, IAF 94-S.3.422.
7. D. P. Schmidt, N. B. Meezan, W. A. Hargus and M. A. Cappelli, Plasma Sources Sci. Technol. 9, 68 (2000).
8. Y. Raitses and N.J. Fisch, Phys. Plasmas 8, 2579 (2001).
9. A. Shirasaki and H. Tahara, J. Appl. Phys. 101, 073307 (2007).
10. J. Lee, W. Choe, K. Chai, Hp3-060 in Bulletin of the Korean Physics Society, 82nd Korean Physical Society Meeting, Pyung Chang, Korea, April 2006.
11. A. Smirnov, Y. Raitses, and N.J. Fisch, J. Appl. Phys. 94, 852 (2003).
12. A. Smirnov, Y. Raitses, and N.J. Fisch, IEEE Trans. Plasma Sci. 34, 132 (2006).
13. A. Fruchtman and A. Cohen-Zur, Appl. Phys. Lett. 89, 111501 (2006).
14. M. Keidar and I. D. Boyd, Appl. Phys. Lett. 87 121501 (2005).

15. Y. Raitses, D. Staack, A. Dunaevsky and N. J. Fisch, *J. Appl. Phys.* 99, 036103 (2006); N. J. Fisch, Y. Raitses, L. Dorf and A. Litvak, *J. Appl. Phys.* 89, 2040 (2001).
16. D. M. Goebel, K. K. Jameson, R. M. Watkins, I. Katz, and I. G. Mikellides, *J. Appl. Phys.* 98, 113302 (2005).

## List of Figures

Fig. 1 Principle of operation of the cylindrical Hall thruster.

Fig. 2 Plume narrowing with the overrun discharge current (OC): Ion flux angular distribution measured for the 2.6 cm and 3 cm CHTs at the discharge voltage of 250 V and the xenon gas flow rate of 4 sccm. The ion flux was measured with a guarding sleeve probe and with zero bias RPA. The centerline is at 0°.

Fig. 3 Ion energy distribution function (IEDF) measured at different angular placements of the RPA. The 3 cm CHT was operated with and without the overrun current (OC) at the discharge voltage of 250 V and the Xenon gas flow rate of 4 sccm.

Fig. 4 The thruster anode efficiency of the 2.6 cm CHT thruster at different discharge voltages (200-350 V) and anode flow rates (2-3 sccm, Xenon). For the overrun current (OC) operation, the open and filled box markers correspond to the anode efficiency and input power values obtained with and without taking into account the additional power ( $\sim 50$  W) used to overrun the discharge current, respectively.

Fig. 5 RPA measurements for the 3 cm CHT (250 V, 4 sccm, Xenon): The total ion current (a) and the half-plume angle (b) (estimated for 90% of the total ion current) with and without the overrun discharge current (OC). The RPA voltage is given with respect to ground. Note that only ions with energies higher than  $eV_{\text{RPA}}$  can reach the RPA collector. The reproducibility of plume measurements was better than 5%.

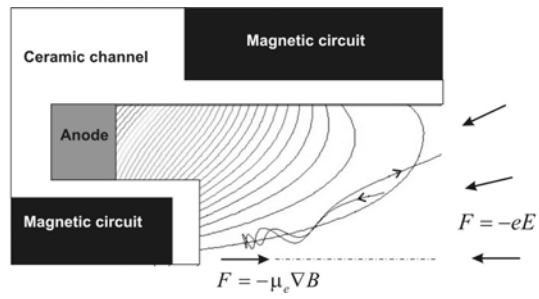


Fig. 1 Principle of operation of the cylindrical Hall thruster.

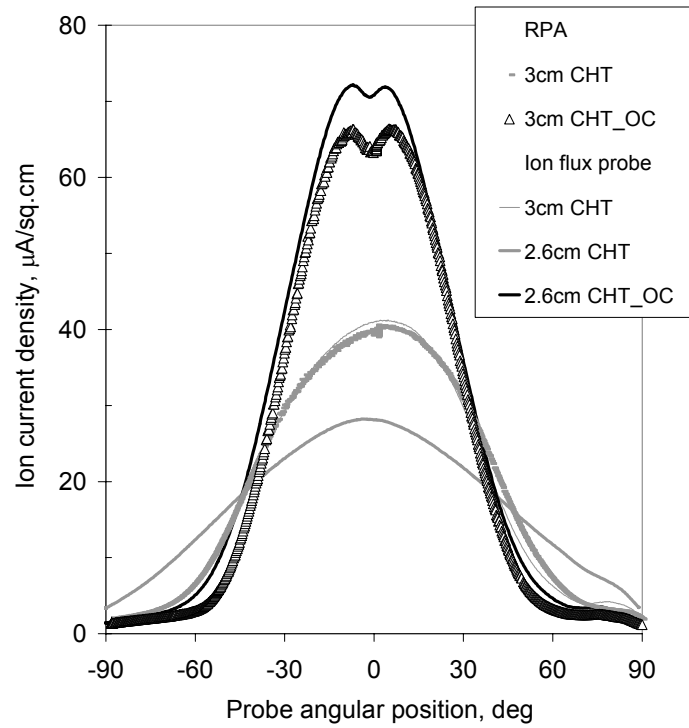


Fig. 2 Plume narrowing with the overrun discharge current (OC): Ion flux angular distribution measured for the 2.6 cm and 3 cm CHTs at the discharge voltage of 250 V and the xenon gas flow rate of 4 sccm. The ion flux was measured with a guarding sleeve probe and with zero bias RPA. The centerline is at 0°.

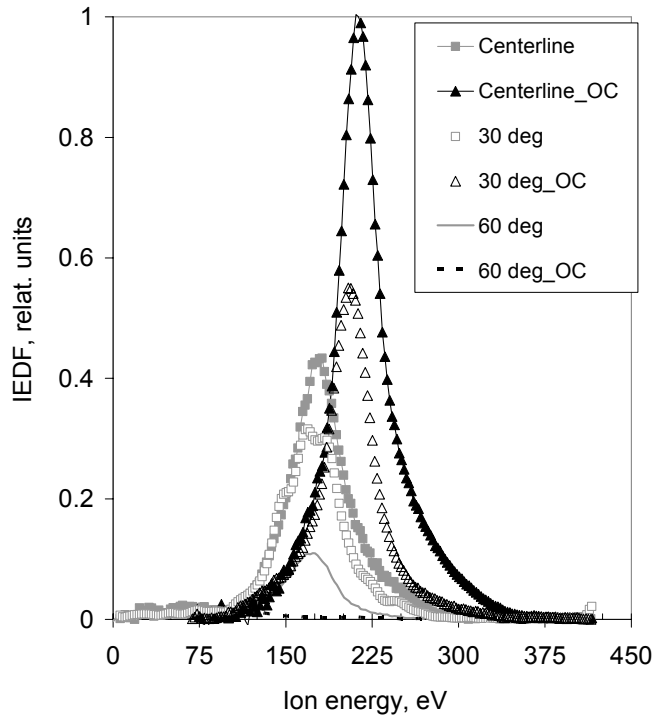


Fig. 3 Ion energy distribution function (IEDF) measured at different angular placements of the RPA. The 3 cm CHT was operated with and without the overrun current (OC) at the discharge voltage of 250 V and the Xenon gas flow rate of 4 sccm.

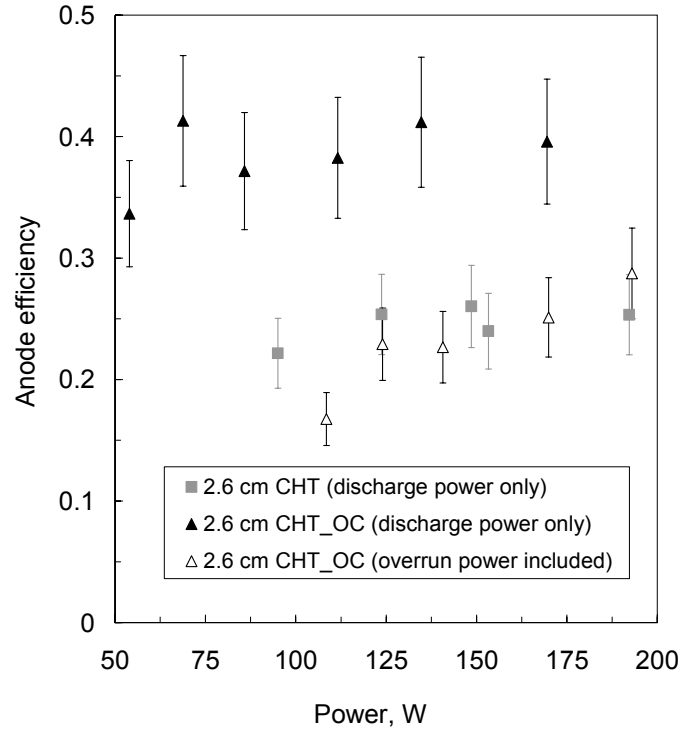


Fig. 4 The thruster anode efficiency of the 2.6 cm CHT thruster at different discharge voltages (200-350 V) and anode flow rates (2-3 sccm, Xenon). For the overrun current (OC) operation, the open and filled box markers correspond to the anode efficiency and input power values obtained with and without taking into account the additional power ( $\sim 50$  W) used to overrun the discharge current, respectively.

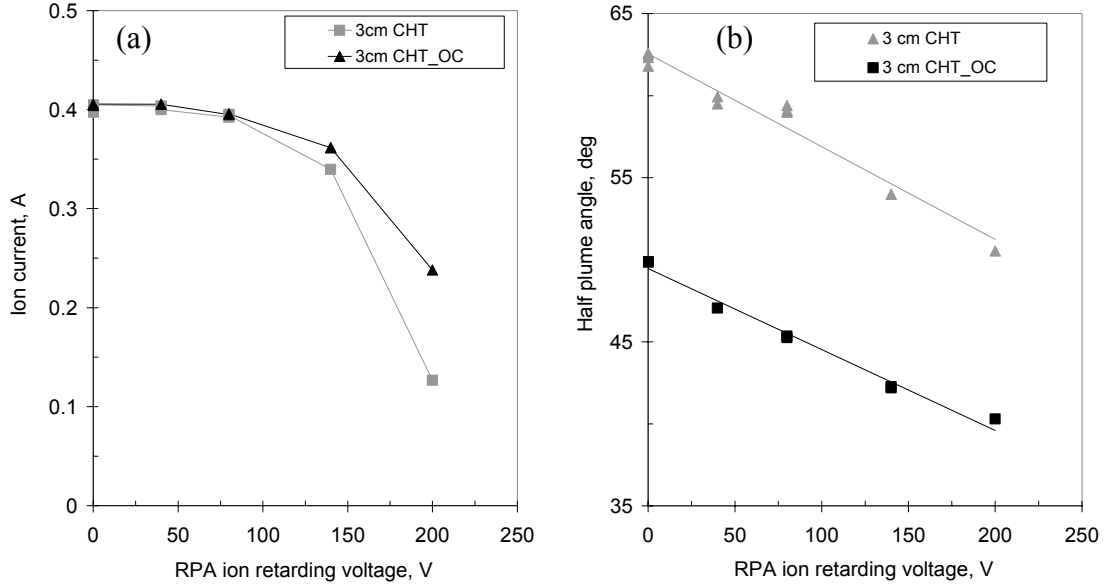


Fig. 5 RPA measurements for the 3 cm CHT (250 V, 4 sccm, Xenon): The total ion current (a) and the half-plume angle (b) (estimated for 90% of the total ion current) with and without the overrun discharge current (OC). The RPA voltage is given with respect to ground. Note that only ions with energies higher than  $eV_{\text{RPA}}$  can reach the RPA collector. The reproducibility of plume measurements was better than 5%.

The Princeton Plasma Physics Laboratory is operated  
by Princeton University under contract  
with the U.S. Department of Energy.

Information Services  
Princeton Plasma Physics Laboratory  
P.O. Box 451  
Princeton, NJ 08543

Phone: 609-243-2750  
Fax: 609-243-2751  
e-mail: [pppl\\_info@pppl.gov](mailto:pppl_info@pppl.gov)  
Internet Address: <http://www.pppl.gov>